Int. J. Heat Mass Transfer. Vol. 17, pp. 429–437. Pergamon Press 1974. Printed in Great Britain

EXPERIMENTS ON HEAT TRANSFER TO TRANSPIRED TURBULENT PIPE FLOWS

G. LOMBARDI*, E. M. SPARROW and E. R. G. ECKERT

Department of Mechanical Engineering, University of Minnesota, Minneapolis, Minnesota 55455, U.S.A.

(*Received* 30 *July* 1973)

Abstract—Local heat transfer results were deduced from measurements on turbulent flow of air in a porous-walled tube. Hydrodynamically developed, room temperature air was ducted to the entrance cross section of the tube, and heated air was injected through the tube wall. The experiments were performed for inlet Reynolds numbers of the main flow ranging from 4000 to about 65 000 and for injection Reynolds numbers (based on the tube diameter and injection velocity) of approximately 25, 50, 100 and 200. The local Nusselt numbers in the presence of injection were generally lower than those for a solid-walled tube, with the reductions being most marked at low values of the local main flow Reynolds number. It was found that the local Nusselt numbers in the downstream region of the tube could be correlated by local parameters, the local main flow Reynolds number and the injection Reynolds number, without separate dependence on the inlet Reynolds number and the axial position. At small values of the inlet Reynolds number and high rates of injection, a partial laminarization of the flow was evidenced by very low values of Nusselt number in the initial portion of the tube.

NOMENCLATURE

c_p, specific heat at constant pressure;
D, internal diameter of porous tube;
h, local heat transfer coefficient;
i, enthalpy per unit mass;
k, thermal conductivity;
$\dot{M}$, mass rate of the main flow;
$\dot{m}$, mass rate of the injected flow per unit length;
Nu, local Nusselt number, hD/k;
Nu_0, fully developed Nusselt number in a solid-walled duct;
Pr, Prandtl number;
q, local heat transfer per unit time and area;
Re_i, inlet Reynolds number of main flow, $4\dot{M}(0)/\mu\pi D$;
Re_{loc}, local Reynolds number of main flow $4\dot{M}(x)/\mu\pi D$;
Re_w, injection flow Reynolds number, DV_w/ν;
T, temperature;
V_w, injection velocity, $\dot{m}/\rho\pi D$;
μ, viscosity;
ν, kinematic viscosity;
ρ, density.

Subscripts

b, bulk;
p, injection-air plenum;
w, wall of porous tube.

*On leave from Departmento de Hidraulica e Saneamento, Escola de Engenharia de São Carlos, São Paulo, Brazil.

INTRODUCTION

HEAT transfer to turbulent boundary layer flows with transpiration at the bounding surface has been studied extensively during the past decade, and a significant body of experimentally based heat transfer information is now available [1, 2]. On the other hand, for turbulent pipe flows with surface transpiration, a search of the literature failed to disclose any experimental results for the heat transfer coefficient. In the present paper, experiments on transpired turbulent pipe flows are described, and results for the local heat transfer coefficient are presented and correlated.

The experiments were performed in a porous circular tube in which both the main flow and the injected flow were air. The injected flow was preheated prior to being introduced into the test section, whereas the main flow entering the test section was at room temperature. The inlet Reynolds number of the main flow ranged from 4000 to 65 000. Four rates of transpiration were employed during the course of the experiments, characterized by injection Reynolds numbers Re_w (see Nomenclature) of approximately 25, 50, 100 and 200. Owing to fluid injection, the main flow Reynolds number increased along the length of the pipe. For the largest and the smallest rates of transpiration, the respective increments in the main flow Reynolds number between the entrance and the exit of the test section were about 18 000 and 2500. The active length of the test section was about 23 pipe diameters.

Local heat transfer coefficients were determined by

evaluating energy balances with measured values of temperature and mass flow. The measured quantities included local wall temperatures, the inlet temperature of the main flow, the temperature in the plenum chamber of the injected flow, and the mass flow rates of the main flow and the injected flow. The heat transfer results were examined from a number of viewpoints, including their dependence on the local main flow Reynolds number, on the injection Reynolds number, and on position along the tube. It was found possible to correlate all the data by a single curve, thereby enabling easy application of the results to operating conditions which differ from those of the present experiments.

The aforementioned literature survey turned up a number of experiments on mass transfer in turbulent duct flows. In the main, these studies were restricted to extremely small values of the transverse velocity at the duct wall. The experiments of Wasan and coworkers [3] on vaporization of acetone and on injection of carbon dioxide into turbulent flow of air in a circular tube were characterized by wall Reynolds numbers comparable to those of the present investigation. Their test section was very short (less than six diameters in length) and only overall mass transfer coefficients are reported, so that direct comparison cannot be made with the present results.

APPARATUS

The experiments were performed in an open loop air flow facility. Dried and filtered air from a building supply system was ducted to the main-flow and injection-flow piping circuits. Each circuit contained a pressure regulator, flow control valve, and orifice flow meter. The main flow pipeline delivered the air to a plenum chamber from which it passed via a sharp-edged entrance into a smooth, seamless brass tube which served as a hydrodynamic development section. The development tube was 90 diameters in length. At its downstream end, it was connected to the test section by a delrin* union which was designed to minimize heat conduction. The diameter of the development tube was selected to be the same as that of the porous test section tube.

Downstream of the orifice meter, the air in the injection-flow pipeline passed through a heater section which consisted of a transite cylinder, 12·5 cm dia and 26·8 cm in length, within which were distributed 15 electrical resistance coils deployed in cross flow to the streamwise direction. To ensure temperature uniformity of the injection air flow, the heater was followed by a length of aluminum pipe filled with copper wool. The heater, the temperature equalization section, and all downstream piping in the injection-flow circuit were wrapped with fiberglass insulation. The heated injection flow was delivered to four inlet ports in the test-section plenum chamber by means of a branching system of flexible hoses.

The test section assembly is pictured schematically in Fig. 1. The porous tube, made of Porostrand porous metal, had an internal diameter of 3·55 cm and a length of about 23·5 diameters. The tube had been fabricated* by winding alternate layers of solid and stranded stainless steel wire on a cylindrical mandrel, wrapping a perforated stainless steel sheet about these layers, and then wrapping a second pair of solid and stranded wires over the perforated sheet. The wires were joined at all points of contact by a sintering operation, the result being a rigid porous tube.

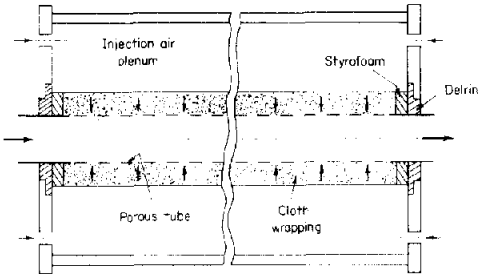

FIG. 1. Schematic of test section assembly.

The wall thickness of the porous tube was only about 0·15 cm. As a consequence, the radial pressure drop experienced by injected fluid in traversing the thickness of the tube wall would be very small. In order to achieve uniform injection all along the length of the tube, the radial pressure drop must be very much larger than any axial variations of pressure along the tube. To ensure uniform injection, the Porostrand tube was tightly wrapped with 80 layers of rayon cloth that had been chosen on the basis of uniformity of thread count. The thickness of the 80 cloth layers was about 1·5 cm. The uniformity of the injected flow had been verified by earlier experiments that were concerned with the velocity field characteristics of transpired turbulent pipe flows [4, 5].

The 5-cm annular gap between the cloth and the external shell of the test section assembly served as the plenum chamber of the injection flow. The heated injection air was introduced into the plenum through four inlet ports, two of which were in the upstream flange and the other two in the downstream flange.

To minimize heat losses and attendant temperature non-uniformities, the entire test section assembly was heavily blanketed with fiberglass insulation. In addition, with the same motivation, the central portion of

*A free machining plastic.

*Bendix Filter Corporation.

the flanges was fabricated from delrin plastic rather than from metal, and disks of styrofoam were used to fill the space between the cloth and the flanges.

The porous tube was instrumented with thermocouples at ten axial stations having coordinate locations $x/D = 0, \frac{1}{2}, 1, 2, 4, 6, 10, 14, 18$ and 23. Four thermocouples were installed at each axial station, respectively at the 12 o'clock, 3 o'clock, 6 o'clock and 9 o'clock angular positions. In order to minimize blockage of the injection flow due to the presence of the thermocouples, small diameter wire was employed (36 gage, diameter of wire = 0·114 mm, diameter of wire and teflon insulation = 0·157 mm). The thermocouples were fabricated from copper and constantan wire and were calibrated prior to their installation. All aspects of the fabrication and installation of the thermocouples were performed with meticulous care and attention to detail, with those operations connected with the installation of the thermocouples being carried out under a microscope.

The first step in the installation of a thermocouple was to machine a shallow crater into the external surface of the Porostrand tube. This was accomplished with a dental drill bit, and the resulting craters were typically 0·2–0·3 mm deep and 0·5 mm dia. The thermocouples were welded into their seats by means of a capacitor discharge, the welding process being performed in a non-oxidizing argon atmosphere. From the junctions, the thermocouple wires were laid along the surface of the Porostrand tube, with one wire from each pair going to the upstream flange and the other wire to the downstream flange.* To avoid interference and overlap between wires from different junctions, the wires were arranged to lie on helical paths on the surface of the tube. Less than 5 per cent of the tube surface was blocked off by the presence of the thermocouple lead wires.

The temperature of the heated air in the injection flow plenum chamber was measured by 16 calibrated copper–constantan thermocouples, also made from 36-gage wire. For the measurement of the entering bulk temperature of the main flow, a calibrated thermocouple probe was installed at the downstream end of the hydrodynamic development tube. The probe station was $4\frac{3}{4}$ tube diameters from the inlet of the porous tube.

Thermocouple outputs were read and recorded by a Digitrend digital millivoltmeter having an accuracy of 1 μV. A strip chart recorder was employed to monitor specified thermocouple outputs in order to identify the onset of steady state operating conditions.

The mass flow rates of the main and injection flows were measured by calibrated orifices in conjunction with water and mercury manometers. The calibration was performed by means of the weigh-tank method, with water as the calibrating fluid and with the upstream and downstream pipelines attached. The orifices were sized so that when employed to meter the main and injection flows, the compressibility correction factors were always within a few per cent of unity. For the lowest rate of injection flow, a calibrated rotameter was employed to meter the flow.

*Except for the thermocouples at $x/D = 23$, where all wires were run to the downstream flange, and for the thermocouples at $x/D = 0$, where all wires were run to the upstream flange.

DATA ANALYSIS

The determination of the local heat transfer coefficient involves the local rate of heat transfer q per unit area and the local wall and bulk temperatures, T_w and T_b, respectively. The methods by which these quantities were deduced from the measured data will now be discussed.

The bulk temperature at any axial station x was evaluated from an overall energy balance on a cylindrical control volume whose length extends from $x = 0$ to $x = x$ and whose radius extends beyond the cloth wrapping into the plenum chamber. In writing the energy balance, it was assumed that axial conduction was negligible, and a similar assumption was made for the axial convection in the porous media.

Let $\dot{M}$ represent the mass flow rate of the main flow at any station x and i_b the bulk enthalpy per unit mass of the main flow at x. In addition, the uniform rate of injection flow per unit length will be denoted by $\dot{m}$ and the enthalpy of the injection air in the plenum chamber by i_p. In terms of these quantities, the energy balance can be written as

$$\dot{M}(x)i_b(x) = \dot{M}(0)i_b(0) + \dot{m}xi_p \tag{1}$$

where the kinetic energy terms have been neglected because their contribution is negligible for the operating conditions of the experiments. Also, a mass balance for the control volume yields

$$\dot{M}(x) = \dot{M}(0) + \dot{m}x. \tag{2}$$

Elimination of $\dot{M}(x)$ from the foregoing and introduction of $\Delta i = c_p \Delta T$ leads to

$$T_b(x) = \frac{\dot{M}(0)T_b(0) + \dot{m}xT_p}{\dot{M}(0) + \dot{m}x}. \tag{3}$$

The entering bulk temperature $T_b(0)$ of the main flow and the air temperature T_p in the injection-flow plenum chamber are measured quantities, as are the flow rates $\dot{M}(0)$ and $\dot{m}$. Therefore, the local bulk temperature $T_b(x)$ can be calculated directly from equation (3).

For the local heat flux q, an annular control volume is employed. This control volume has an axial length dx, an inner radius which coincides with the inner

radius of the porous tube, and an outer radius which extends into the injection-flow plenum chamber. The energy balance is written under the assumption that the temperature of the injection air passing through the Porostrand tube is the same as the temperature T_w of the tube wall and that the aforementioned assumptions about axial conduction and convection continue to apply. Then,

$$q\pi D(\mathrm{d}x) + \dot{m}(\mathrm{d}x)i_w = \dot{m}(\mathrm{d}x)i_p \tag{4}$$

and after replacement of enthalpies by temperatures

$$q = \frac{\dot{m}c_p(T_p - T_w)}{\pi D}. \tag{5}$$

Since $\dot{m}$, T_p, and T_w are all measured quantities, q is readily evaluated from equation (5).

A local heat transfer coefficient and local Nusselt number can then be evaluated from

$$h = q/(T_w - T_b), \quad Nu = hD/k. \tag{6}$$

After substitution of q from equation (5), there follows

$$Nu = \frac{\dot{m}c_p(T_p - T_w)}{\pi k\ (T_w - T_b)} \tag{7}$$

from which the Nusselt number can be calculated directly from measured quantities.

An alternate form of the Nusselt number expression can be written by introducing the injection Reynolds number Re_w defined as

$$Re_w = \frac{DV_w}{\nu} = \frac{\dot{m}}{\mu\pi}, \quad V_w = \frac{\dot{m}}{\rho\pi D} \tag{8}$$

where V_w is the injection (or blowing) velocity. With equation (8), the Nusselt number expression becomes

$$Nu = Re_w Pr \frac{(T_p - T_w)}{(T_w - T_b)}. \tag{9}$$

Since the experimental runs were parameterized by Re_w, the local Nusselt number results were actually evaluated from equation (9).

In the forthcoming presentation of results, it will be advantageous to make use of the local main flow Reynolds number Re_{loc} as one of the correlating parameters. This Reynolds number is based on the local mass flow rate $\dot{M}(x)$ of the main flow, so that

$$Re_{loc} = 4\dot{M}(x)/\mu\pi D. \tag{10}$$

It then follows from equations (2) and (8) that

$$Re_{loc} = Re_i + 4(x/D)Re_w \tag{11}$$

where Re_i is the Reynolds number of the main flow at the inlet of the porous tube,

$$Re_i = 4\dot{M}(0)/\mu\pi D. \tag{12}$$

It is seen from equation (11) that Re_{loc} increases linearly along the length of the porous tube. The most downstream measuring station in the present experiments was at $x/D = 23$, and the local Reynolds number at that cross section exceeded Re_i by about 18 000 for $Re_w = 197$ and by 2300 for $Re_w = 25$.

Fluid property variations did not play a major role in the data reduction since the experiments were performed with moderate temperature differences. Typically, the entering bulk temperature of the main flow was about 20°C and the air temperature in the injection-flow plenum chamber was about 50°C. The viscosity appearing in the Reynolds numbers Re_i, Re_{loc}, and Re_w was evaluated at the mean of the inlet and outlet bulk temperatures. The value of Prandtl number used in evaluating the Nusselt number from equation (9) was 0·7.

As was described earlier in the paper, the tube wall temperature was measured at four equally spaced circumferential locations at each axial station. The quantities $(T_p - T_w)$ and $(T_w - T_b)$ were evaluated at each circumferential location. Typically, these quantities varied by about 5 per cent about the respective circumferential average. For the evaluation of the local Nusselt number from equation (9), circumferential average values were used. In a few special cases, specifically for small main flow Reynolds numbers ($Re_i < 10\,000$) and the highest rate of injection ($Re_w = 197$), the circumferential variations were somewhat larger than those noted above. In these cases, the values of $(T_p - T_w)$ were substantially less than 1°C, so that circumferential irregularities as small as 0·1°C would give rise to relatively large percentage variations.

The temperatures measured by the 16 thermocouples in the injection-air plenum chamber were generally within a few tenths of a degree of their mean value. However, for the lowest rate of injection ($Re_w = 25$), there was evidence of stratification in the plenum chamber, with a vertical temperature spread of about 1½°C. The stratification did not cause significant circumferential variations in $(T_p - T_w)$ and $(T_w - T_b)$.

RESULTS AND DISCUSSION

Local Nusselt numbers were deduced from the experimental data for inlet Reynolds numbers Re_i between 4000 and 67 000, for injection Reynolds numbers Re_w of 25, 51, 101 and 197 and at axial positions x/D between 1 and 23. The results will first be presented in a generalized form that should be most useful for applications. Then, the separate influences of local main flow Reynolds number, injection Reynolds number, and axial position will be examined.

In seeking a generalized representation of the results, correlating parameters were sought which would enable the Nusselt number to be evaluated directly (i.e. without interpolation) at any operating condition

within the range investigated. Since Nu depends on Re_i, Re_w and x/D (or, alternatively, on Re_{loc}, Re_w and x/D), it might be expected that all of these quantities would appear explicitly, thereby giving rise to a correlation of complex form. Fortunately, as demonstrated in Fig. 2, it was found possible to correlate the data over most of the operating range in terms of a relationship between only two quantities, Nu/Nu_0 and Re_w/Nu_0. The meaning of these correlating parameters and the significance of Fig. 2 will now be discussed.

The data shown in Fig. 2 and the correlation resulting therefrom are restricted to $Re_{loc} \geqslant 10000$. This limitation is prompted by the fact that at lower Reynolds numbers, the turbulence is not fully developed. Consequently, even for flows in solid-walled ducts, the Nusselt numbers for the low Reynolds number turbulent range are not well represented by the predictive equations for $Re \geqslant 10000$. Furthermore, in the presence of wall transpiration, the Nusselt numbers for low Reynolds number flows display a

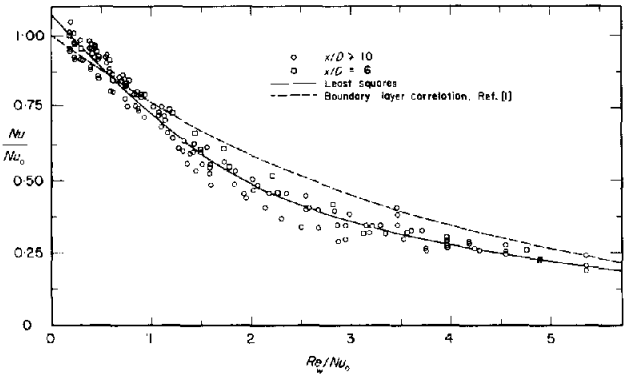

FIG. 2. General correlation of local Nusselt number results.

The local Nusselt number Nu appearing on the ordinate of Fig. 2 is that for transpired turbulent flow, whereas Nu_0 is the fully developed Nusselt number for turbulent flow in a solid-walled tube. Both Nu and Nu_0 correspond to the same local main flow Reynolds number Re_{loc}; that is, Nu_0 is evaluated at a Reynolds number equal to the local Reynolds number that corresponds to Nu. The abscissa parameter, Re_w/Nu_0, involves both Re_{loc} (via Nu_0) and Re_w.

The circular data points that are plotted in the figure are for $x/D \geqslant 10$. These data do not show a separate dependence on x/D. The square points are for $x/D = 6$. Although these points generally lie near the high side of the band of data, they fall within the range of the scatter. With decreasing x/D, a separate dependence on x/D was evident. These findings suggest that sufficiently far downstream from the inlet cross section, the local Nusselt number is almost completely determined by local conditions, i.e. Re_{loc} and Re_w, and is relatively independent of Re_i and x/D. This conclusion will be reaffirmed later when the data are examined from another viewpoint.

Figure 2 may, therefore, be applied to determine the local Nusselt number at any $x/D \geqslant 6$, with only Re_{loc} and Re_w needed as input information. The value of Re_{loc} is used in the evaluation of Nu_0.

different behavior than do those for the higher Reynolds number flows, as will be indicated shortly.

For computational convenience, least square representations have been fitted to the data in Fig. 2 and are shown therein as a solid line. The equations of the least squares line are

$$\frac{Nu}{Nu_0} = 1{\cdot}074 - 0{\cdot}3910\left(\frac{Re_w}{Nu_0}\right) + 0{\cdot}0454\left(\frac{Re_w}{Nu_0}\right)^2 \qquad (13)$$

for $0 \leqslant (Re_w/Nu_0) \leqslant 1{\cdot}71$ and

$$\frac{Nu}{Nu_0} = \frac{1{\cdot}364}{1 + 0{\cdot}7(Re_w/Nu_0)} - 0{\cdot}0830 \qquad (14)$$

for $(Re_w/Nu_0) \geqslant 1{\cdot}71$. As Re_w approaches zero, equation (13) reduces to $Nu/Nu_0 = 1{\cdot}074$ rather than to 1·0 as might be expected. Reasons for this deviation will be discussed in a subsequent paragraph, following comments about Nu_0.

For Nu_0, analytical predictions based on the model of Sparrow, Hallman and Siegel [6] were used since they appear to have been accorded good acceptance [7, 8]. The Nu_0 values for $Pr = 0{\cdot}7$ and for the Reynolds number range between 10000 and 100000 are listed in Table 1.

Table 1. Nu_0 values for $Pr = 0{\cdot}7$

$Re \times 10^{-3}$	10	15	20	30	40	50	75	100
Nu_0	32·3	42·7	52·3	70·0	86·4	101·9	138·1	171·7

The tabulated values of Nu_0 are actually for the uniform wall heat flux boundary condition, but it is well established that the precise nature of the thermal boundary condition is a second order effect for thermally developed pipe flows.

The aforementioned extrapolation of the present results to $Re_w = 0$, which yielded $Nu/Nu_0 = 1{\cdot}074$, is an altogether satisfactory outcome. A seven per cent level of agreement between analysis and experiment for turbulent heat transfer is generally regarded as being very good. Indeed, this level of agreement lends confidence to the experimental techniques and data reduction procedures that were employed. That the extrapolated Nusselt number of the experiments exceeded Nu_0 is also reasonable, since the porous tube, by its nature, possessed a certain degree of roughness which could have produced augmentation.

The correlating parameters employed in Fig. 2 were motivated by Kays' correlation of heat transfer results for the transpired turbulent boundary layer on a flat plate [1]. Although it was not possible to use the boundary layer correlating parameters directly, similar parameters were constructed for the pipe flow problem, with the successful outcome given in Fig. 2. For purposes of comparison, Kays' correlation line has been translated into the present parameters and is plotted as a dashed line in Fig. 2. The agreement between the boundary layer correlation and the present pipe flow correlation is fairly good.

The separate influences of the various independent parameters were masked by the compact correlation given in Fig. 2. These separate influences will now be examined. In Fig. 3, the local Nusselt number results are plotted against the local Reynolds numbers Re_{loc}. The data arrange themselves into groups that are parameterized by Re_w. The blackened symbols are for $x/D \geqslant 10$, whereas the half open and the open symbols correspond, respectively, to $x/D = 6$ and $x/D = 4$. The dashed and dot-dashed lines appearing near the top of the figure represent results for thermally developed heat transfer in solid-walled tubes.

Inspection of the figure indicates that injection (i.e. increasing values of Re_w) can cause significant reductions in the local Nusselt number. The influence of injection becomes increasingly marked at low values of the local Reynolds number. On the other hand, at high values of the local Reynolds number, the main flow is much less sensitive to injection. As Re_w decreases, the Nusselt number results display an orderly

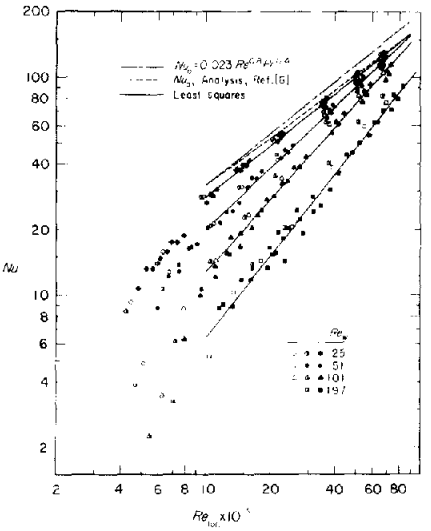

FIG. 3. Variation of local Nusselt number with local Reynolds number.

approach to the predictive equations for the no blowing case. This behavior lends further confidence to the conduct of the experiments.

Further examination of the figure indicates that for $Re_{loc} \geqslant 10\,000$, the data exhibit a regular pattern which can be represented as a straight line for each value of Re_w. In this range, there is no evidence of a separate dependence on x/D for axial positions where $x/D \geqslant 10$. The data for $x/D = 6$ lie near the upper fringe of the scatter band whereas that for $x/D = 4$ generally lie somewhat higher. It thus appears that the local Nusselt number can be regarded as depending only on the local Reynolds number and on Re_w when $x/D \geqslant 6$. This finding supports a similar conclusion that was deduced from Fig. 2.

The results for $Re_{loc} \geqslant 10\,000$ were correlated by the equation

$$Nu = C(Re_{loc})^n \tag{15}$$

where C and n are given in Table 2. Straight lines representing equation (15) and Table 2 have been plotted in Fig. 3 for $Re_{loc} \geqslant 10\,000$.

Table 2. Values of C and n for equation (15)

Re_w	C	n
25	$1{\cdot}96 \times 10^{-2}$	0·788
51	$3{\cdot}39 \times 10^{-3}$	0·942
101	$4{\cdot}97 \times 10^{-4}$	1·10
197	$8{\cdot}59 \times 10^{-5}$	1·22

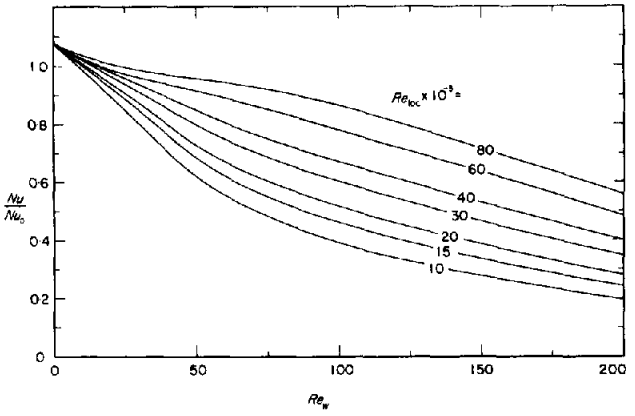

FIG. 4. Variation of local Nusselt number with injection Reynolds number.

For $Re_{loc} < 10\,000$, the data tend to slump off relative to the straight line correlations. This behavior may well be the result of a partial laminarization as was observed by Pennell [5] in his turbulence measurements.

A somewhat different perspective on the results of Fig. 3 can be obtained by examination of Fig. 4, where Nu/Nu_0 is plotted as a function of the injection Reynolds number for parametric values of the local main flow Reynolds number. In constructing this figure, the Nusselt numbers were evaluated from equation (15) and Nu_0 was taken from Table 1. At $Re_w = 0$, Nu/Nu_0 was plotted as 1·074 in accordance with the findings of Fig. 2.

From Fig. 4, it is seen that the Nusselt number decreases monotonically with increasing injection at any given value of the local Reynolds number. Flows having small local Reynolds numbers are much more affected by injection than are flows with higher Reynolds numbers. Reductions in the local Nusselt number by a factor of five are seen to be possible.

The variation of the local Nusselt number with axial position along the tube will now be examined, and Figs. 5–7 have been prepared for this purpose. Both for economy of space and to give perspective, each figure contains results for several inlet Reynolds numbers Re_i covering a fairly wide range. For each Re_i, axial distributions are presented for injection Reynolds numbers Re_w of 25, 51, 101 and 197. As an aid to clarity, one set of data in each figure is plotted using blackened symbols.

From an inspection of the figures, a number of trends can be identified.* At the higher inlet Reynolds num-

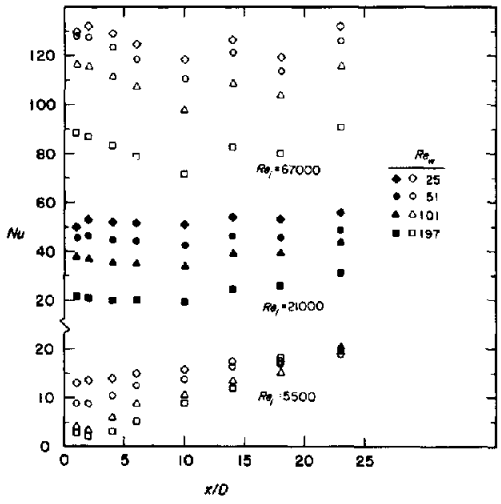

FIG. 5. Variation of local Nusselt number with axial position for $Re_i = 67\,000$, 21 000 and 5500.

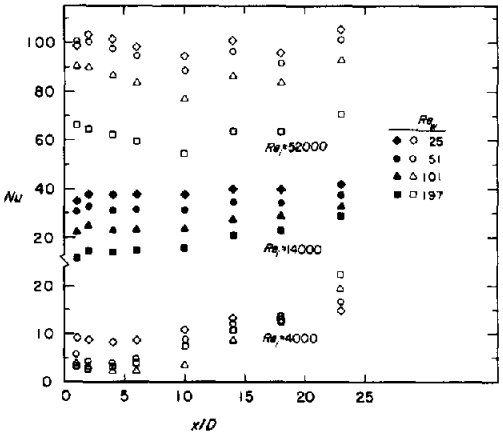

FIG. 6. Variation of local Nusselt number with axial position for $Re_i = 52\,000$, 14 000 and 4000.

*It appears that the data point at $x/D = 14$ is consistently high in all cases. The identification of trends is simplified if this data point is envisioned as lowered by 5–7 per cent.

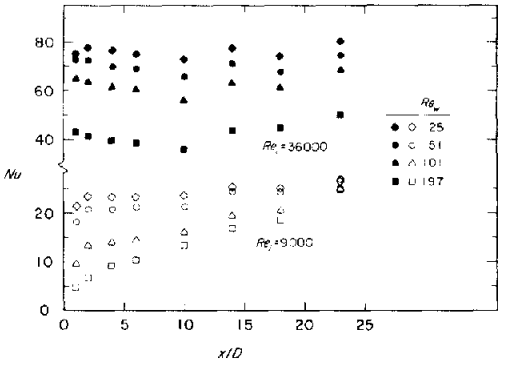

FIG. 7. Variation of local Nusselt number with axial position for $Re_i = 36000$ and 9000.

bers, there is an initial decrease in Nusselt number with x/D, indicative of a thermal entrance region. The extent of the Nusselt number variation in the entrance region is smaller than that encountered in solid-walled ducts. Farther downstream, the Nusselt number increases with x/D due to the progressive increase of the local Reynolds number with downstream distance.

At intermediate values of the inlet Reynolds number, manifestations of the entrance region appear to diminish, whereas the trend of increasing Nusselt number with x/D in the downstream region continues in force.

For small values of inlet Reynolds number, very low values of the Nusselt number are encountered at small x/D, especially at the higher rates of injection. This is believed to be a manifestation of partial laminarization of the main flow due to injection. Such a partial laminarization has already been observed by Pennell in connection with an investigation of the velocity field [5]. In the downstream region, the effect of the progressive increase in local Reynolds number is very strongly manifested by the marked increase of the Nusselt number with x/D.

The combination of a low inlet Reynolds number and a high rate of injection gives rise to large relative changes in local Reynolds number. Thus, for example, when $Re_i = 4000$ and $Re_w = 197$, the local Reynolds number at $x/D = 23$ is about 22000. On the other hand, for the same Re_i but with $Re_w = 25$, the local Reynolds number is 6300 at $x/D = 23$. The merging and subsequent crossing of the data for the different Re_w values is due to the just-mentioned marked differences in local Reynolds number.

CONCLUDING REMARKS

The fact that the local Nusselt number results for $x/D \geqslant 6$ can be correlated by local parameters suggests that away from the inlet, the temperature field passes through a sequence of locally fully developed states as x/D increases. From the standpoint of analysis, this means that it is unnecessary to seek solutions which begin at $x = 0$ and span the entire range of x/D. Rather, a local fully developed model can be employed.

For applications, it may be of interest to be able to predict the local wall temperature T_w of the porous-wall tube. From equation (9), it follows that

$$T_w = \frac{T_p + (Nu/Re_w Pr)T_b}{1 + (Nu/Re_w Pr)}. \tag{16}$$

The local Nusselt number is provided by the correlations described earlier in the paper (e.g. Fig. 2), whereas the local bulk temperature is obtained from equation (3). Since both the air temperature T_p in the injection-flow plenum and the injection Reynolds number Re_w would be known, then T_w is calculable from equation (16).

Acknowledgement Scholarship support accorded to G. Lombardi by the Fundação de Amparo à Pesquisa do Estado de São Paulo is gratefully acknowledged. The research was supported by the Power Branch of the office of Naval Research.

REFERENCES

1. W. M. Kays, Heat transfer to the transpired turbulent boundary layer, *Int. J. Heat Mass Transfer* **15**, 1023–1044 (1972).
2. A. I. Leont'ev, Heat and mass transfer in turbulent boundary layers, in *Advances in Heat Transfer*, Vol. 3, Academic Press, New York (1966).
3. D. T. Wasan, W. O. Jones and G. L. Von Behren, Entry region mass transfer in turbulent pipe flow, *A.I.Ch.E. Jl* **17**, 300–308 (1971).
4. R. M. Olson and E. R. G. Eckert, Experimental studies of turbulent flow in a porous circular tube with uniform fluid injection through the tube wall, *J. Appl. Mech.* **33**, 7–17 (1966).
5. W. T. Pennell, E. R. G. Eckert and E. M. Sparrow, Laminarization of turbulent pipe flow by fluid injection, *J. Fluid Mech.* **52**, 451–464 (1972).
6. E. M. Sparrow, T. M. Hallman and R. Siegel, Turbulent heat transfer in the thermal entrance region of a pipe with uniform heat flux, *Appl. Scient. Res.* **A7**, 37–52 (1957).
7. R. L. Webb, A critical evaluation of analytical solutions and Reynolds analogy equations for turbulent heat and mass transfer in smooth tubes, *Wärme- und Stoffübertragung* **4**, 197–204 (1971).
8. W. M. Kays and H. C. Perkins, Forced convection, internal flow in ducts, in *Handbook of Heat Transfer*, Section 7. McGraw-Hill, New York (1973).

EXPERIENCES SUR LE TRANSFERT THERMIQUE POUR DES ECOULEMENTS TURBULENTS DANS LES TUBES POREUX

Résumé—Des résultats de transfert thermique local sont déduits de mesures pratiquées sur un écoulement turbulent d'air dans un tube à paroi poreuse. Développé hydrodynamiquement, de l'air à la température ambiante est conduit jusqu'à la section droite d'entrée du tube, et de l'air chauffé est injecté à travers la paroi du tube. Les expériences ont été conduites pour des nombres de Reynolds de l'écoulement principal à l'entrée compris entre 4000 et 65 000 et pour des nombres de Reynolds à l'injection (basés sur le diamètre du tube et la vitesse d'injection) approximativement égaux à 25, 50, 100 et 200. Les nombres de Nusselt locaux en présence d'injection sont généralement inférieurs à ceux relatifs au tube à paroi imperméable, les réductions étant d'autant plus marquées que le nombre de Reynolds local de l'écoulement principal est faible. On a trouvé que les nombres de Nusselt locaux peuvent être reliés aux paramètres locaux, le nombre de Reynolds local pour l'écoulement principal et le nombre de Reynolds à l'injection, sans dépendance distincte vis à vis du nombre de Reynolds à l'entrée et de la position axiale.

Pour des faibles valeurs du nombre de Reynolds à l'entrée et des débits d'injection élevés, une laminarisation partielle de l'écoulement est mise en évidence par de très faibles valeurs du nombre de Nusselt dans la première partie du tube.

UNTERSUCHUNGEN DES WÄRMEÜBERGANGS AN PORÖSEN ROHREN BEI TURBULENTER STRÖMUNG

Zusammenfassung—In prösen Rohren und turbulenter Luftströmung wurde der örtliche Wärmeübergang aus Messungen bestimmt. Luft mit Raumtemperatur im hydrodynamisch eingelaufenen Zustand wurde an die Eintrittsöffnung des Rohres herangeführt, während erhitzte Luft durch die Rohrwand eingeblasen wurde. Die Untersuchungen wurden im Reynolds-Zahlbereich von 4000 bis 65 000 der Hauptströmung durchgeführt. Die Reynolds-Zahlen der durch die Rohrwand eingeblasenen Luft (bezogen auf den Rohrdurchmesser und die Einblasgeschwindigkeit) betrugen etwa 25, 50, 100 und 200. Die örtlichen Nusselt-Zahlen bei Einblasung waren im allgemeinen niedriger als die für das dichte Rohr. Die größten Verringerungen traten bei kleinen Reynolds-Zahlen des örtlichen Hauptstromes auf. Die örtliche Nusselt-Zahl in Gebieten stromabwärts konnte mit Hilfe lokaler Parameter, sowie der örtlichen Reynolds-Zahl des Hauptstromes und der des eingeblasenen Stroms, ohne getrennte Abhängigkeit von der Reynolds-Zahl am Eintritt und der axialen Position wiedergegeben werden. Bei kleinen Reynolds-Zahlen am Eintritt und hohen Einblasraten wird an Hand der sehr niedrigen Nusselt-Zahlen eine teilweise Laminarisierung der Strömung im vorderen Teil des Rohres bewiesen.

ЭКСПЕРИМЕНТЫ ПО ПЕРЕНОСУ ТЕПЛА К ТУРБУЛЕНТНОМУ ПОТОКУ В ПРОНИЦАЕМОЙ ТРУБЕ

Аннотация — Получены результаты по локальному теплообмену на основе измерений в турбулентном потоке воздуха в трубе с пористыми стенками. Гидродинамически развитый поток воздуха комнатной температуры поступал во входной участок трубы, а нагретый воздух вдувался через стенку. Эксперименты проводились для значений чисел Рейнольдса основного потока от 400 до 65 000 и для чисел Рейнольдса для вдува около 25, 50, 100 и 200, отнесенных к диаметру трубы и скорости вдува. Локальные числа Нуссельта при вдуве были, в общем, меньше чисел Нуссельта для трубы со сплошными стенками, причём это уменьшение было наиболее заметным при малых значениях локального числа Рейнольдса основного потока. Найдено, что локальные числа Нуссельта в области вниз по потоку можно обобщить с помощью локальных параметров, а именно, локального числа Рейнольдса основного потока и числа Рейнольдса вдува, без учёта зависимости от числа Рейнольдса на входе и положения вдоль трубы. При малых числах Рейнольдса на входе и высоких скоростях вдува очень малые значения числа Нуссельта в начальном участке трубы свидетельствуют о частичной ламинаризации потока.